Research Paper

Lipidomic and metabolic profiling of plasma and plasma-derived extracellular vesicles by UHPLC-MS/MS

Daisuke Saigusa[1,2*], Takeshi Honda[3], Yuko Iwasaki[1], Koji Ueda[4], Eiji Hishinuma[2,5], Naomi Matsukawa[2], Akira Togashi[6,7,8], Noriyuki Matsutani[9], Nobuhiko Seki[3*]

[1] Laboratory of Biomedical and Analytical Sciences, Faculty of Pharma-Science, Teikyo University, 2−11−1 Kaga, Itabashi-ku, Tokyo 173−8605, Japan
[2] Department of Integrative Genomics, Tohoku Medical Megabank Organization, Tohoku University, 2−1 Seiryo-machi, Aoba-ku, Sendai 980−8573, Japan
[3] Division of Medical Oncology, Department of Internal Medicine, Teikyo University School of Medicine, 2−11−1 Kaga, Itabashi-ku, Tokyo 173−8606, Japan
[4] Project for Realization of Personalized Cancer Medicine, Cancer Precision Medicine Center, Japanese Foundation for Cancer Research, 3−8−31 Ariake, Koto, Tokyo 135−8550, Japan
[5] Advanced Research Center for Innovations in Next-Generation Medicine, Tohoku University, 2−1 Seiryo-machi, Aoba-ku, Sendai 980−8573, Japan
[6] Nippon Boehringer Ingelheim Co., Ltd., ThinkPark Tower, 2−1−1 Osaki, Shinagawa-ku, Tokyo, Japan
[7] Molecular Profiling Research Center for Drug Discovery, National Institute of Advanced Industrial Science and Technology (AIST), 2−3−26 Aomi, Koto-ku, Tokyo 135−0064, Japan
[8] Japan Biological Informatics Consortium (JBIC), TIME24 Bldg. 10th Floor, 2−4−32 Aomi, Koto-ku, Tokyo 135−8073, Japan
[9] Dept. of Surgery, Teikyo University School of Medicine Mizonokuchi Hospital, 5−1−1 Futako, Takatsu-ku, Kawasaki 213−8507, Japan

Abstract Extracellular vesicles (EVs) are secreted from donor cells that bind to receptors on receiving cells to mediate signal transduction. EVs contain nucleic acids, proteins, miRNAs and small molecules, including lipid species and other metabolites. These molecules are likely functional mediators and have potential as candidate disease biomarkers and/or therapeutic targets. However, EV-selective isolation and the optimal extraction of small molecules are essential to observe the variation in EV molecules, and a more detailed classification of lipid species is required for lipidomic profiling in EVs. Here, we examined methanol precipitation to extract a wide polarity range of small molecules from isolated EVs of human plasma by kit-based metabolic and lipidomic profiling using ultrahigh-performance liquid chromatography triple quadrupole tandem mass spectrometry and multivariate analyses. A total of 278 and 379 molecules were identified in EVs and plasma, respectively. The contents of triglycerides consisting of polysaturated fatty acids were significantly higher in EVs than in plasma, whereas the contents of cholesterol esters were lower in EVs. This method of EV lipidomic profiling may be essential to reveal the function of EVs and utilize them for future biomarker discovery in the clinical field.

Key words: extracellular vesicles, lipidome, metabolome, UHPLC-MS/MS

*** Corresponding authors**

Daisuke Saigusa
Laboratory of Biomedical and Analytical Sciences
Faculty of Pharma-Science, Teikyo University
2−11−1 Kaga, Itabashi-ku, Tokyo 173−8605, Japan
Tel: +81−3−3946−8069
E-mail: saigusa.daisuke.vf@teikyo-u.ac.jp

Nobuhiko Seki
Division of Medical Oncology, Department of Internal Medicine,
Teikyo University School of Medicine
2−11−1 Kaga, Itabashi-ku, Tokyo 173−8606, Japan
Tel: +81−3−3964−1211
E-mail: nseki@med.teikyo-u.ac.jp

Received: July 8, 2022. Accepted: October 13, 2022.
Epub November 15, 2022.
DOI: 10.24508/mms.2022.11.007

Introduction

The smaller size of secreted extracellular vesicles (EVs) are 50−150 nm in diameter that are thought to reflect the characteristics of the original cell, as their surface contains lipids and proteins derived from the cell membrane, while their interior contains nucleic acids and proteins derived from the cell, and to be involved in cell−cell communication mechanisms in physiological and pathological tissues[1]. The EVs secreted from donor cells bind to receptors on the surface of receiving cells, and the contents of EVs taken up by the receiving cell mediate signal transduction[2]. For instance, it has been reported that the intravenous preadministration of EVs derived from lung metastatic cancer cells to mice followed by the intravenous administration of bone metastatic cancer cells increases lung metastasis, even though the cells themselves are not capable of lung metastasis[3]. The role of exosomal molecules in the central nervous system in neurodegenerative diseases, such as Alzheimer's disease and Parkinson's disease, has also been demonstrated in a previous report[4]. Therefore, exosomal components are likely to act as functional mediators and could be candidates for disease biomarkers and/or therapeutic targets.

The metabolome is the group of small-molecule substrates and products of metabolism, including a wide range of metabolites, such as amino acids, biogenic amines, sterols, fatty acids, and lipid species, that drive essential cellular functions, such as energy production and storage and signal transduction. The metabolome can derive from microorganisms, as well as from xenobiotic, dietary and other exogenous sources, and directly reflects phenotypic changes in the human body[5,6]. Therefore, metabolic profiling to characterize these molecules in circulating biofluids and tissues is a promising approach to identify biomarkers for disease prediction, progression, and prognosis and to investigate the role of small molecules in systems biology and disease expression[7,8]. Various analytical platforms provide information on the metabolic phenotypes of individuals or populations, which can be applied to personalized medicine for drug development or to public healthcare for biomarker discovery[9,10]. In fact, metabolic and lipidomic profiling by mass spectrometry (MS)-based technologies has identified potential biomarkers that gave us functional and/or new information on disease expression using several biospecimens. Moreover, biomarker discovery targeting the differences in lipid species in disease has become a growing scientific field with the recent development of MS-based analytical technologies[11]. Therefore, the lipidomic profiling of not only general biospecimens but also EVs is an interesting way to identify new potential biomarkers that are differentially expressed with the progression of disease[12,13]. For instance, the most abundant lipid classes were found to be triglycerides (TGs), phosphatidylcholines (PCs) and sphingomyelins (SMs), which represented 53.5−56.2%, 35.5−39.4% and 3.5−6.2% of all lipids in EVs, respectively, and high abundances of exosomal sphingosines and certain other lipids were strongly associated with hepatocellular carcinoma by means of MS-based lipidomic profiling[14]. In contrast, 3′-UMP, palmitoleic acid, palmitaldehyde, and isobutyl decanoate were significantly associated with oesophageal squamous cell carcinoma[15]. Therefore, both exosomal lipids and metabolites have potential as biomarkers. In addition, the lipidomic characterization of EVs isolated from human plasma using various MS techniques has previously been reported[16]. Since this study was performed on EVs in plasma or serum, it was necessary to use EV-selective isolation and the optimal extraction of small molecules as pretreatment methods to observe the variations in molecules contained in EVs specifically, and a more detailed classification of lipid species, such as the saturation of fatty acids, is required to understand the difference in lipidomic profiling between plasma and EVs[17].

In this study, we first obtained EV samples isolated from plasma by means of an EV-selective extraction method developed previously[18]. Next, the extraction conditions for detecting a wide range of small molecules, including lipid species and other components, in EVs were optimized to determine the quantitative values of each molecule by ultra-high-performance liquid chromatography triple quadrupole tandem mass spectrometry (UHPLC-MS/MS) using hierarchical clustering heatmaps, principal component analysis (PCA) and volcano plot analyses. We then investigated differences in the quantitative values of the small molecules, focusing on the lipid species derived from plasma and its EVs to clarify the characteristic lipid species by using a PAI chart, correlation plots and volcano plot analysis.

Materials and Methods

Reagents

Acetonitrile, chloroform, isopropanol, and methanol were purchased from Kanto Chemical Co., Inc. (Tokyo Japan) for the LC/MS analyses. Formic acid, ammonium

formate (1 mol/L), phenyl isothiocyanate (PITC) and MagCapture™ Exosome Isolation Kit PS were purchased from FUJIFILM Wako Pure Chemical Corporation (Osaka, Japan). Purified water was obtained from a Milli-Q Gradient system (Millipore, Billerica, MA, USA). Ethanol was purchased from Nacalai Tesque (Kyoto, Japan). Pooled normal human plasma (NorPla) and Na EDTA (IPLA-N, Lot: 26393) were purchased from Innovative Research, Inc. (Novi, MI, USA).

EV extraction and transmission electron microscopy (TEM) analysis

EVs were isolated from NorPla (200 μL) by the Tim4-affinity method, and the MagCapture™ Exosome Isolation Kit PS was used according to the manufacturer's instructions (NorEVs)[18]. In brief, 0.6 mg of streptavidin magnetic beads bound with 1 μg of biotinylated mouse Tim4-Fc was added to 10 K supernatant supplemented with 2 mM $CaCl_2$, and the mixture was rotated overnight at 4°C. The beads were washed three times with 1 mL of washing buffer (20 mM Tris-HCl, pH 7.4, 150 mM NaCl, 0.0005% Tween 20, 2 mM $CaCl_2$), and the bound sEVs were eluted with elution buffer (20 mM Tris-HCl, pH 7.4, 150 mM NaCl, 2 mM EDTA) (TBS). The isolated EVs in the buffer (10 μL) were dried on freshly glow-discharged 200 mesh carbon-coated Cu TEM grids (NISSIN EM, Tokyo, Japan), negatively stained with TI blue (NISSIN EM), and observed using an H-7650 TEM (Hitachi High-Tech Corp., Tokyo, Japan) operated at 80 kV. The image of the visualized EVs was captured by the software.

Sample preparation procedure for analysis of the EV lipidome and metabolome

The final EV extract (NorEVs) was in TBS (100 μL), and 50% or 80% methanol in water or 100% methanol (500 μL) was added to NorEV samples (n=3 each). Each sample was mixed for 30 s, sonicated for 5 min, and evaporated under vacuum for 20 min. The residue was frozen at −80°C and lyophilized for 18 h. Then, the sample was dissolved (20 μL, water/acetonitrile, 50/50, v/v%), applied to a 96-well plate, and analyzed by the MxP® Quant 500 kit (Biocrates Life Sciences AG, Innsbruck, Austria). NorPla (10 μL) was also applied to the plate. A blank, calibration standard and Biocrates quality control were applied to the plate as optimal internal standards (ISs). All of the preparation procedures followed the kit protocol, and the detailed UHPLC-MS/MS method and conditions were as previously described[8].

Analytical conditions of UHPLC-MS/MS

The UHPLC system consisted of dual pumps (ACQUITY UPLC H-Class, Waters, Wilmslow, Manchester, UK) and an autosampler with a column compartment (ACQUITY UPLC I-Class), and multiple reaction monitoring (MRM) was performed with the Xevo® TQ-XS system (Waters). The optimal UHPLC-MS/MS and flow injection analysis (FIA)-MS/MS modes with all ionization parameters, ion transfer voltages/temperatures and the detection of *m/z* pairs of precursor and product ions in MRM mode for 628 molecules were automatically set using the method in the kit. The representative 106 molecules, including amino acids, amino acid-related metabolites, bile acids, biogenic amines, cresol, fatty acids, hormones, indole derivatives, nucleobases and vitamins, were detected in the samples via UHPLC-MSMS using an analytical column, and 521 lipid species (such as acylcarnitines (ACs), ceramides (Cers), hexosylceramides (HexCers), dihydroceramides, cholesterol esters (CEs), lysophosphatidylcholines (LPCs), PCs, SMs, diacylglycerols (DGs), TGs, and one hexose (mixture of sugars) were detected in samples via flow injection analysis (FIA)-MS/MS. The number of carbon and double bonds of PCs were the sum of two fatty acids separated by two acyls, “aa,” or including ether, “ae,” and our method characterized one acyl chain and its TG properties. The other two chains were described by the summed carbon bond and double bond numbers.

Data processing

The data were collected by MassLynks 4.2 software (Waters). Quantified values (μmol/L) were calculated according to the manufacturer's protocol using MetIDQ Oxygen software (Biocrates Life Sciences AG). The data sheet from a file in Excel 2018 was exported from the software and highlighted in 4 colours according to the kit criteria: purple:＜limit of detection; yellow: IS out of range; light blue:＜lower limit of quantification or＞upper limit of quantification; and green: quantified. The values coloured green and light blue were selected. The lipid species and other metabolites that satisfied specific criteria were selected: the species that were detected in all triplicate samples in NorPla or NorEVs with a coefficient of variation (CV) less than 30%. The extracted molecules were subjected to further multivariate analysis by MetaboAnalyst

5.0 (https://www.metaboanalyst.ca/). The statistical analysis, creation of a PAI chart, and correlation analyses were performed by GraphPad Prism 8.4.3.

Results and Discussion

EV extraction and TEM analysis

The MagCapture™ exosome isolation kit was recently developed to select EVs based on binding with PS, including PS on the membrane of the EV surface, and utilized for the analysis of EV-specific functions[18]. We first observed the size of EVs by TEM, and most EVs were under 50 nm, which excluded large EVs (Fig. 1), thereby achieving consistency with the size of EVs in previous publications. Therefore, the metabolites extracted from EVs were estimated for small EVs.

Several sample preparation procedures have been established using organic solutions, such as methanol, ethanol, acetonitrile, isopropanol and chloroform/methanol. Therefore, we first profiled the exosomal small molecules by an isolation kit with wide polarity coverage by means of methanol precipitation[19]. We then prepared 50, 80 and 100% methanol (500 μL, each) because the sample EV extract solution was an existing buffer solution (100 μL), whereas the estimated content in the organic solution was 42, 68, and 80% methanol. We proposed that research on the methodology for isolating EVs and extracting exosomal molecules is essential, and more careful design for method optimization, especially using organic solutions, is required for the future study of biomarker discovery targeting lipids or metabolites.

We prepared 200 μL samples of plasma in this study due to the limited sample volume (maximum 200 μL, each) of the MagCapture™ exosome isolation kit. We then examined the volume of plasma for the detection of metabolites from exosomal samples. The total concentration of metabolites in each group increased with the volume of plasma, and 600 μL of plasma seemed suitable for analysis (data not shown). Therefore, more than 200 μL of plasma should be prepared for a second assay of the concentrations of targeted exosomal metabolites in future studies.

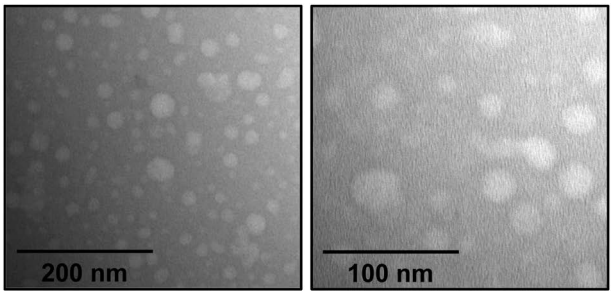

Fig. 1. Transmission electron microscopy images of EVs derived from plasma.
Scale bar=100 or 200 nm.

Comparison of the exosomal molecular profiles in EVs isolated from human plasma and extracted with different concentrations of methanol

A total of 264, 278, or 264 small molecules were stably detected from isolated EVs by UHPLC-MS/MS with high accuracy of quantification based on the kit criteria. More than 250 molecules were lipid species, and 9 were other metabolites. All detected molecules are listed in Supplemental Table S1.

We then analysed the curated data with MetaboAnalyst for hierarchical cluster heatmap analysis. Two large clusters of TGs (TG group 1 and TG group 2) and clusters of PCs or LPCs could be observed in the heatmap (Fig. 2). For instance, a higher concentration of TGs (groups 1 and 2) was detected in the EVs extracted by using a solution of 80% methanol, whereas a lower concentration was detected using 50% or 100% methanol. TGs may have hydrophobic, hydrophilic or both types of acyl chains in the compound structure. In fact, TGs that have polysaturated fatty acids (PUFAs), such as TG (20:5_34:1), TG (18:1_32:3) and TG (20:2_34:2), were significantly higher in concentration due to hydrophilic acyl chains.

Similarly, a higher concentration of TG (group 1) clusters consisting of PUFAs, such as 18:2 and 18:3 of TG, could be observed by using 50% methanol. In contrast, a lower concentration of TG (group 2) clusters consisting of saturated fatty acids (SFAs), such as 14:0, 16:0, 18:0, or monounsaturated fatty acids (MUFAs), such as 16:1 or 18:1 of TG, could be observed by using 50% methanol. Therefore, the reduction in TG levels by extraction with 50% methanol was due to the lower extraction capacity for the hydrophobic type of fatty acids, SFAs and MUFAs of TGs.

Although a higher concentration of PCs could be observed in the heatmap by extraction with 50% or 100% methanol than with 80% methanol due to the hydrophilicity of the phosphate group, there are many characteristic clusters of PCs that depend on the fatty acid saturation, such as TGs. However, a higher concentration of LPCs was detected by extraction with 100% methanol. This result was due to the capacity of the extracting solution, which had a

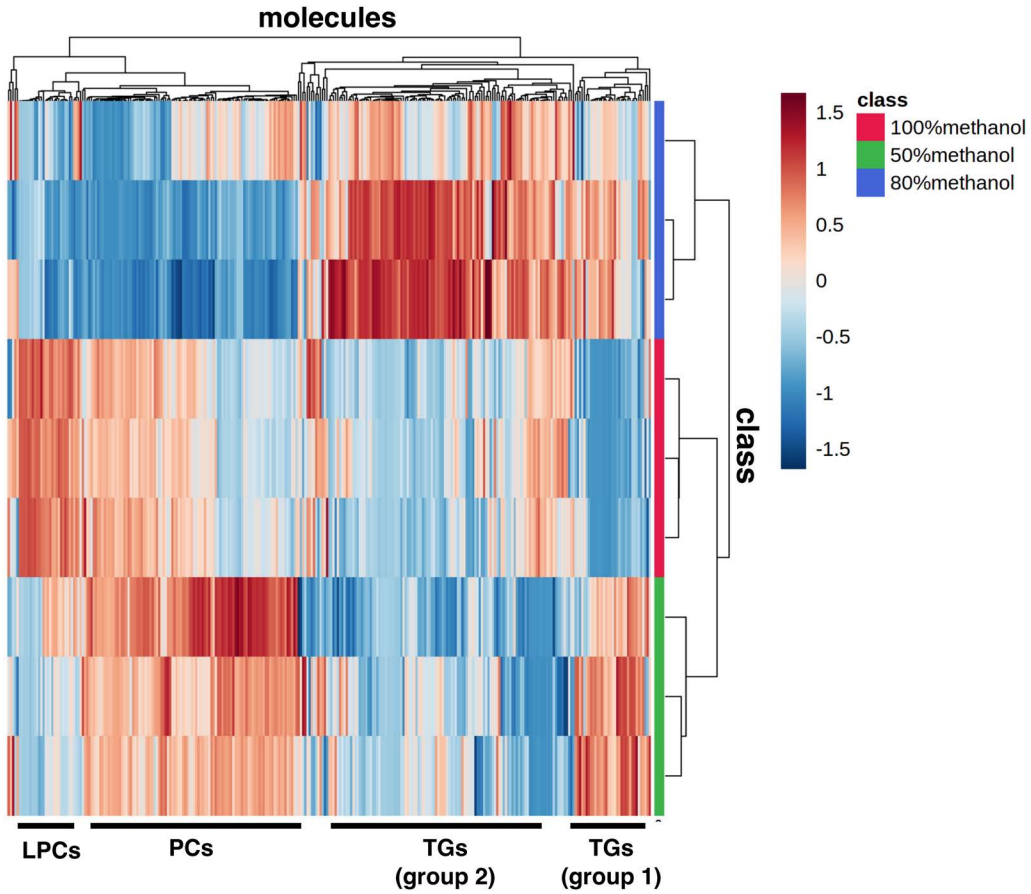

Fig. 2. Hierarchical clustering heatmaps of molecules extracted by using 50, 80 or 100% methanol from EVs isolated from human plasma.

Quantile and Pareto scaling were used for sample normalization and data scaling. The distance was measured by Pearson and clustered by average. The relatively higher and lower rates are shown in deeper red and blue, respectively. The three classes, 50, 80 and 100% methanol (n=3, each), are shown in green, blue and red, respectively.

higher capability of dissolving LPC into 100% methanol, instead of a lower dissolving rate of TGs in 100% methanol. We then researched the XlogP3-AA (logP) values of metabolites on PubChem (https://pubchem.ncbi.nlm.nih.gov/) to estimate the relationship between the solvent property and the hydrophobicity. Lower logP values of LPC (5.6 to 12.1) were observed, and PCs, including PUFAs, had similar values. However, the logP values of TG were clearly higher than those of LPC and PC. Although the present results show one aspect of choosing lipid extraction conditions, the ability to identify the detailed difference between isomers of lipid species is limited. Therefore, further studies using in silico prediction methods are needed to estimate such differences. All molecular lists in the hierarchical cluster heatmap (expanding version of Fig. 2) are shown in Supplemental Figure S1.

We next investigated PCA and volcano plot analysis to observe which molecules contributed to the differences in extraction efficiency among the three groups. The score plot of PCA indicated that PC1 and PC2 explained 88.8% of the variation and characteristic distribution among the three groups (Fig. 3). Notably, the characteristic components extracted with 50% and 80% methanol were similar to each other and different from those extracted with 100% methanol.

Therefore, we first compared the molecules between the 80% methanol and 100% methanol extracts by volcano plot, and 57 molecules were selected with a fold change (FC) threshold$>$1.5 and a P value threshold$<$0.05 in Fig. 4(a, top panel) and are listed in Supplemental Table S2. The statistical significance was calculated using the MetaboAnalyst algorithm[20], and the molecules that were not quantified or not detected in one group exhibited larger variation, log2 (FC)<-2 and $2<$log2 (FC). Several species of TGs were significantly higher on the volcano plot after extraction with 80% methanol, while multiple species of

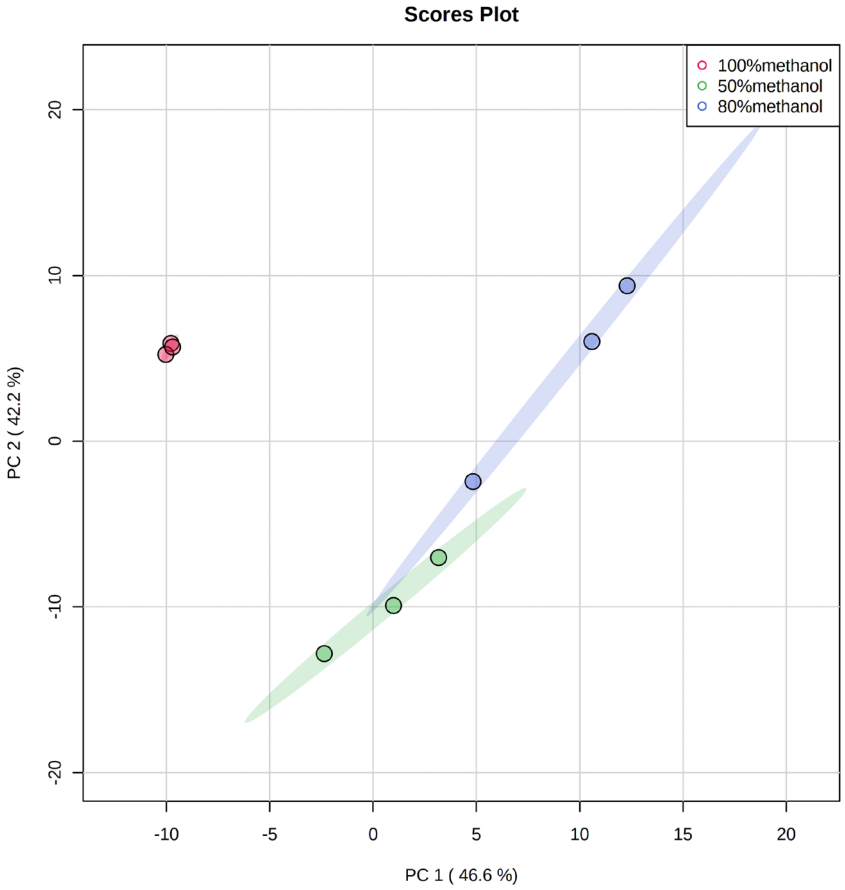

Fig. 3. Score plot of principal component analysis among three groups: 50, 80 or 100% methanol extraction.
The green, blue and red dots represent 50, 80 and 100% methanol extraction, respectively.

LPCs were significantly lower, as mentioned above.

We next compared the molecules between the 50% methanol and 100% methanol extracts by volcano plot in Fig. 4 (b, middle panel), and 41 molecules were significantly higher or lower in the 80% methanol extract (Supplemental Table S2). In particular, the difference in TGs reflected the difference in fatty acid molecular species contained in TGs, as described above. However, there were no significant molecular species of PCs and LPCs, whereas the levels of HexCers and Cers were significantly higher in 50% methanol. Furthermore, we compared the molecules between the 50% methanol and 80% methanol extracts by volcano plot in Fig. 4 (c, bottom panel), and 42 molecules were significantly higher or lower in 80% methanol than in 100% methanol (Supplemental Table S2). TGs were significantly lower in 50% methanol. Although some species of PCs and LPCs were significantly higher in 50% methanol than in 80% methanol, they had relatively low abundances in the EVs. Notably, the abundances of multiple species of HexCers were significantly higher in 50% methanol. The higher hydrophilicity might be attributable to the hexose group(s), which were estimated to have lower values of logP than Cers.

In general, lipid species are extracted with methanol, chloroform, and other organic solvents to cover as many lipid classes as possible[21], and the complexity of choosing the mixture ratio of organic solvents for extracting small molecules was previously reported by Bligh and Dyer[22]. However, the first molecular profile screening in EVs should cover the wide range of polarities not only of lipid species but also of polar metabolites. We therefore selected methanol precipitation based on previous publications[23,24], and a total of 296 metabolites were detected in the EV samples by kit analysis for widely targeted molecules. In fact, the most abundant lipid species measured using the metabolome kit was TGs, and the total concentration of TGs in the 80% methanol extract was significantly higher than the others. The concentration of PCs was also higher in EVs, and both 50% methanol and 80% methanol could extract PCs better than 100% methanol. On the other hand, LPCs were present at lower concentrations in 80% methanol than in the other methanol concentrations; nevertheless, LPCs and their metabolites are essential lipid mediators involved in

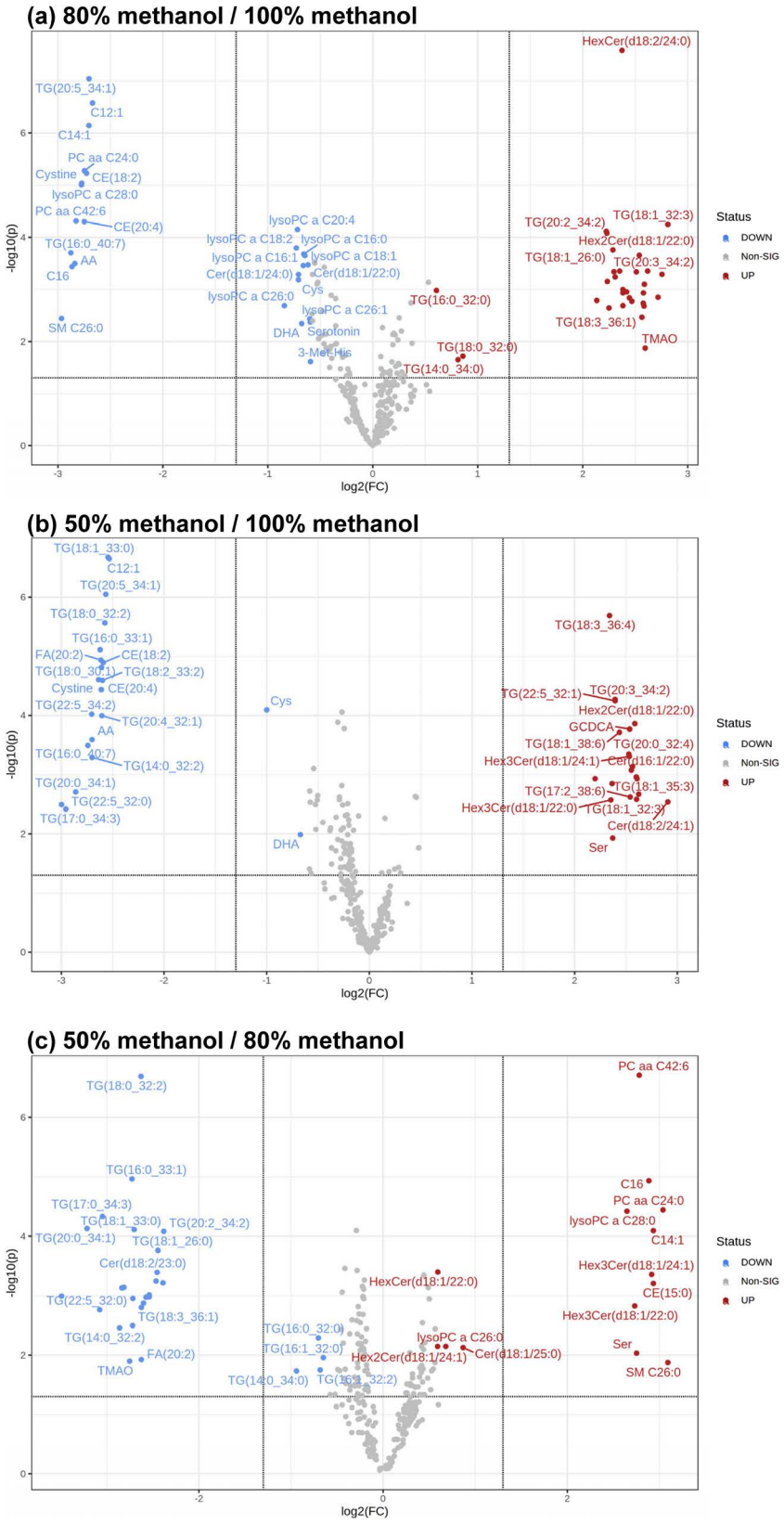

Fig. 4. Volcano plots of detected molecules between (a) 80% methanol and 100% methanol extraction; (b) 50% methanol and 100% methanol extraction; (c) 50% methanol and 80% methanol extraction.

The red and blue dots with their compound names indicate significantly higher and lower contents, respectively, between the two groups.

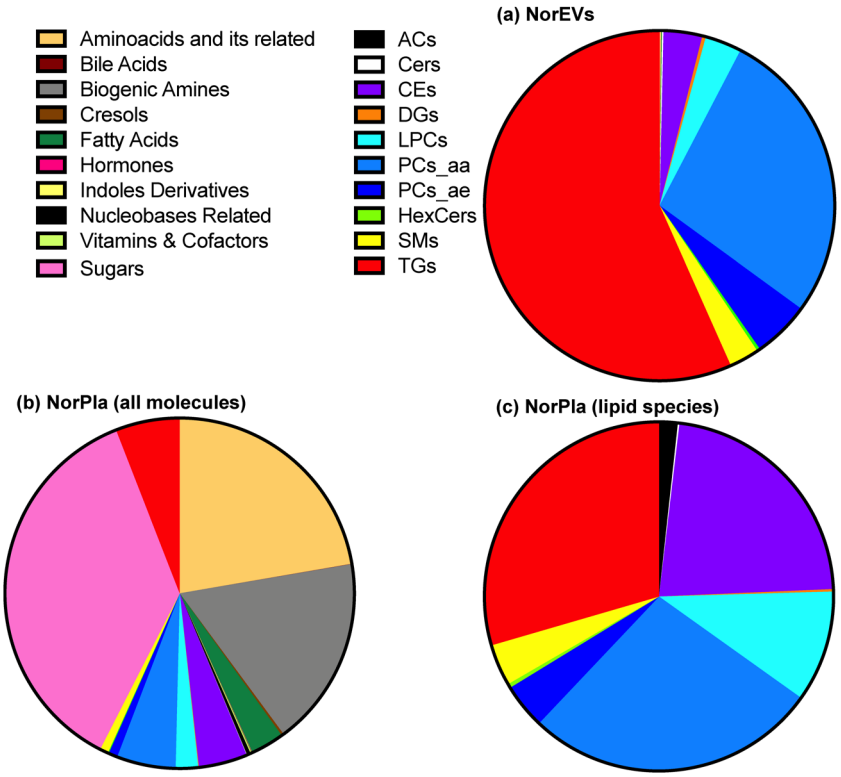

Fig. 5. PAI chart of the concentrations of classified molecules as contributions to the in total concentration (μmol/L).
(a) Molecules in EVs isolated from normal human plasma (NorEVs, total concentration: 1,107 μmol/L); (b) molecules in plasma (NorPla, total concentration: 12,059 μmol/L); (c) lipid species extracted from NorPla data (total concentration: 2,422 μmol/L)

disease expression and progression[25,26].

Differences in exosomal and plasma lipidomes and metabolomes

A total of 379 molecules were stably detected in NorPla, whereas 278 molecules were detected in NorEVs by kit profiling using UHPLC-MS/MS (Supplemental Table S3). The total concentrations of small molecules in NorPla and NorEVs were 12,059±459 μmol/L and 1,107±54 μmol/L, respectively, and the metabolites in NorEVs were found to be approximately ten times lower than those in NorPla. We then discriminated the abundances of small molecules according to the primary classes in the kit, and the results are displayed in a PAI chart (Fig. 5). The lipid species represented a higher percentage in NorEVs than in NorPla, as shown in Fig. 5 (a, upper panel). Notably, TGs and PCs were highly abundant in EVs, which was consistent with a previous publication[16].

In contrast, amino acids and their related biogenic amines, mainly lactic acid and sugars, were present at higher concentrations in NorPla, as shown in Fig. 5 (b, bottom left panel). These differences in metabolites between plasma and EVs have been reported; however, these molecules could not be detected by previous GC-MS/MS analysis owing to the very low abundances of amino acids in EVs, whereas their abundances are higher in plasma[27]. In the present study, although most amino acids could not be detected in all samples, even those derived from 600μL plasma, corresponding to the method in the previous study, some specific amino acids, such as cysteine, could be detected by UHPLC-MS/MS. Cysteine and cystine are key molecules in energy metabolism and are related to the elimination of oxidative stress in organisms[28]. Exosomal amino acid metabolism is still not well understood. We therefore focused on the variation in lipid species contained in NorEVs and NorPla. A total of 304 lipid species were selected, and their total concentration in NorPla was 2,422±33 μmol/L, which was found to be twice the concentration in NorEVs. The PAI chart of lipid species in NorPla is shown in Fig. 5 (c, bottom right panel).

Interestingly, CEs were more abundant in NorPla than NorEVs, whereas TGs and PCs were more abundant in both NorPla and NorEVs. Free cholesterol in the blood is esterified on the surface of HDL by the action of lecithin choles-

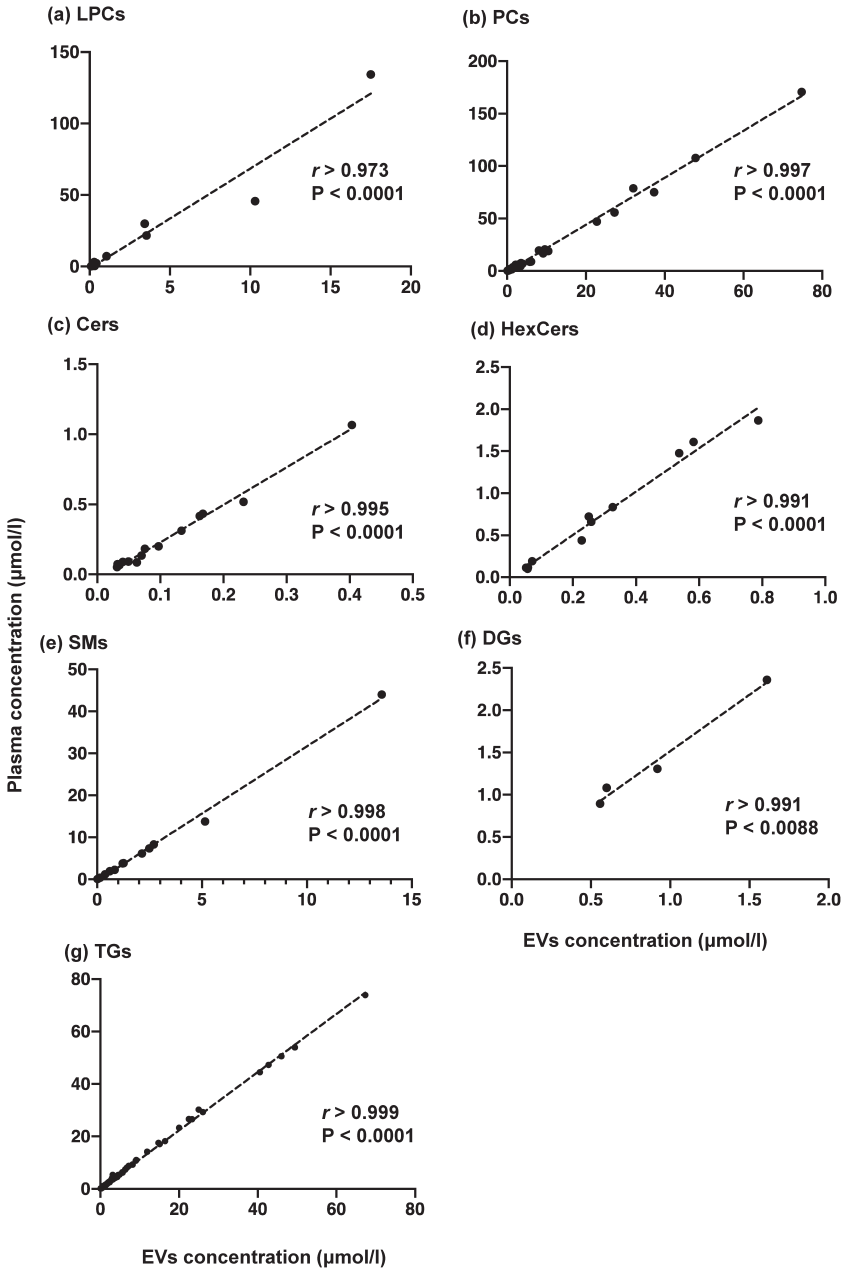

Fig. 6. Correlation of concentration between plasma and EV molecules.

(a) Lysophosphatidylcholines, LPCs; (b) phosphatidylcholines, PCs; (c) ceramides, Cers; (d) hexosylceramides, HexCers; (e) sphingomyelins, SMs; (f) diacylglycerols, DGs; (g) triacylglycerols, TGs.

The Pearson correlation coefficient (*r*) and P value are shown for each lipid class plot.

terol or free cholesterol in the blood[29]. The CEs are mainly produced by cholesterol acyltransferase and are highly abundant in the very low-density lipoproteins (VLDL) and low-density lipoproteins (LDL) in the blood. On the other hand, large amounts of TGs are contained or accumulated in chylomicrons in blood, whereas TGs are lower in HDL and LDL. Therefore, the content of TGs and CEs directly indicates the ratio of lipoproteins in blood and EV differences.

Previously, it has been demonstrated that ceramide-enriched EVs in the blood plasma are increased in mice with stress-induced major depressive disorder[30], and the adiponectin/T-cadherin system enhances EV biogenesis and secretion, leading to a decrease in cellular ceramides[31]. In fact, EV secretion was increased by overexpression of the ceramide synthase neutral sphingomyelinase[32]. Therefore, exosomal ceramide has an important role in mediating cell signals from donor cells. In contrast, the exosomal concentration of Cer was lower than that in plasma in the present study. In general, ten to hundreds of samples were prepared to profile the molecules in EVs[33], and the concentrations of

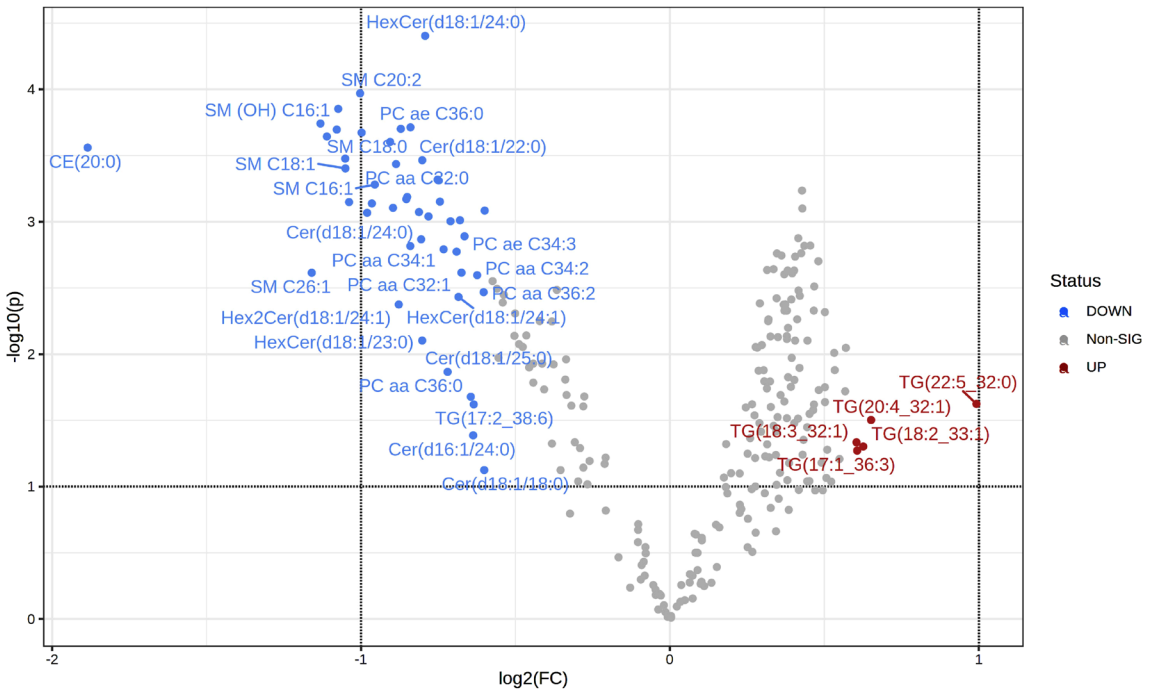

Fig. 7. Volcano plots of lipid species detected in EVs and plasma.
The red and blue dots with their compound names indicate significantly higher and lower contents, respectively, between the two groups.

EV lipid classes were approximately 2−12 times lower than those in plasma[16]. Although the number of plasma EVs derived from healthy and unhealthy individuals should be examined to confirm the Cer concentration in future studies, the value of EV/plasma Cer may have potential as a biomarker.

We next investigated the correlation of concentration in NorEVs and NorPla in each lipid class. The concentrations of the lipid classes (number of species) in NorEVs for LPCs (11), PCs (68), Cers (14), HexCers (11), SMs (13), DGs (4) and TGs (139) were highly correlated (r>0.973) with those in NorPla (Fig. 6). Interestingly, the concentration of TGs in EVs was similar to that in the original plasma (Fig. 6g), whereas PCs and the other lipid species were 1.5−8.0 times lower.

We then investigated the lipid species with the greatest contributions to the difference between NorEVs and NorPla by volcano plot analysis (Fig. 7). The values were median normalized and palate scaled by MetaboAnalyst. TGs were significantly higher in NorEVs than NorPla, notably, those TGs with PUFAs. EVs mediate cell signals to inhibit the effects of oxidative stress[34], and PUFAs react with antioxidants to reduce oxidative stress[35]. Therefore, EVs may accumulate PUFAs in TGs to reduce the effects. A detailed examination focusing on the antioxidative effect to reveal the function of EV TGs is needed.

On the other hand, CE (20:0), SMs, Cers, and HexCers were more abundant in NorPla, whereas PCs with SFA or MUFA were found to be significantly less abundant in NorPla than in NorEVs. The results indicated that the composition of exosomal lipid species was different from that of the original plasma and corresponded to the previous exosomal lipidomic analysis[16]. Indeed, although LPCs were significantly lower in NorEVs than in NorPla, we excluded the LPCs from the comparative analysis to prevent an artefact due to the lower extraction efficiency of 80% methanol for LPC extraction from NorEVs. The original volcano plot is shown in supplemental Figure S3.

In this study, we discussed the quantification of total metabolites and lipids in plasma and EVs. Although the determination method followed the protocol of the MxP Quant 500 Kit, which was established based on the standard operating procedure for method validation, the quantified values of lipid species should be evaluated with other methodologies[36]. Therefore, for the major lipids and metabolites, recovery rates need to be proven for plasma and EV samples by additive recovery studies in the future.

In summary, exosomal small molecules, including lipid species and metabolites derived from human plasma, have been analysed previously[25,27]. However, the detailed varia-

tion in lipid species remained unknown. We demonstrated the difference in lipid species in TGs, focusing on SFAs, MUFAs and PUFAs, and the present results are essential to reveal the function of EVs and utilize them for future biomarker discovery in the clinical field.

Author Contributions

Conceptualization, D.S., A.T., No.M. and N.S.; methodology, D.S., Y.I., K.U., E.H. and Na.M.; software, D.S., E.H., and T.H.; data curation, D.S., T.H., K.U., E.H. and N.M.; writing—original draft preparation, D.S.; writing—review and editing, D.S., T.H, A.T., Na.M. A.T., No.M. and N.S.; visualization, D.S., Y.I.; supervision, A.T., No.M. and N.S; funding acquisition, D.S., K.U., A.T., No.M. and N.S. All authors have read and agreed to the published version of the manuscript.

Acknowledgements

This work was supported in part by the Tohoku Medical Megabank Project from MEXT, the Japan Agency for Medical Research and Development (AMED; under grant numbers JP20km0105001 and JP21tm0124005), the Project for Promoting Public Utilization of Advanced Research Infrastructure (MEXT), and the Sharing and Administrative Network for Research Equipment (MEXT). A part of this work was also supported by KAKENHI Grant Number JP20H03374 [D.S.], AMED LEAP under Grant Number J200001087 [D.S.], and a grant from Boehringer Ingelheim [K.U., N.S.]. We thank the members of the Central Laboratory of Teikyo University for their support in performing the TEM analysis.

Conflict of Interest

NS received personal fees as honoraria from Lily Japan, AstraZeneca K.K., MSD Oncology, Chugai Pharmaceutical, Taiho Pharmaceutical, Pfizer Japan Inc., Ono Pharmaceutical, Nippon Boehringer Ingelheim Co., Ltd., and Bristol-Myers Squibb, Japan, and research funding from AstraZeneca K.K. and Nippon Boehringer Ingelheim Co., Ltd.

References

1) Song Q, Yu H, Han J, Qiang Lv JL, Yang H: Exosomes in urological diseases—Biological functions and clinical applications. *Cancer lett* 215809, 2022.
2) O'Brien K, Breyne K, Ughetto S, Laurent LC, Breakefield XO: RNA delivery by extracellular vesicles in mammalian cells and its applications. *Nat Rev Mol Cell Biol* 21(10): 585−606, 2020.
3) Hoshino A, Costa-Silva B, Shen TL, Rodrigues G, Hashimoto A, et al: Tumour exosome integrins determine organotropic metastasis. Nature 527(7578): 329−335, 2015.
4) Fan Y, Chen Z, Zhang M: Role of exosomes in the pathogenesis, diagnosis, and treatment of central nervous system diseases. *J Transl Med* 20(1): 291, 2022.
5) Johnson CH, Patterson AD, Idle JR, Gonzalez FJ. Xenobiotic metabolomics: Major impact on the metabolome. *Annu Rev Pharmacol Toxicol* 52: 37−56, 2012.
6) Johnson CH, Ivanisevic J, Siuzdak G. Metabolomics: Beyond biomarkers and towards mechanisms. *Nat Rev Mol Cell Biol* 17(7): 451−459, 2016.
7) Nicholson JK, Holmes E, Kinross JM, Darzi AW, Takats Z, et al: Metabolic phenotyping in clinical and surgical environments. *Nature* 491(7424): 384−392, 2012.
8) Saigusa D, Matsukawa N, Hishinuma E, Koshiba S: Identification of biomarkers to diagnose diseases and find adverse drug reactions by metabolomics. *Drug Metab Pharmacokinet* 37: 100373, 2021.
9) Holmes E, Wilson ID, Nicholson JK: Metabolic phenotyping in health and disease. *Cell* 134(5): 714−717, 2008.
10) Wishart DS: Emerging applications of metabolomics in drug discovery and precision medicine. *Nat Rev Drug Discov* 15(7):473−484, 2016.
11) Köfeler HC, Ahrends R, Baker ES, Ekroos K, Han X, et al: Recommendations for good practice in MS-based lipidomics. *J Lipid Res* 62: 100138, 2021.
12) Morioka S, Nakanishi H, Yamamoto T, Hasegawa J, Tokuda E, et al: A mass spectrometric method for in-depth profiling of phosphoinositide regioisomers and their disease-associated regulation. *Nat Commun* 13(1): 83, 2022.
13) Scavo MP, Depalo N, Tutino V, De Nunzio V, Ingrosso, et al: Exosomes for diagnosis and therapy in gastrointestinal cancers. *Int J Mol Sci* 21(1): 367, 2020.
14) Sanchez JI, Jiao J, Kwan SY, Veillon L, Warmoes MO, et al: Lipidomic profiles of plasma exosomes identify candidate biomarkers for early detection of hepatocellular carcinoma in patients with cirrhosis. *Cancer Prev Res (Phila)* 14(10): 955−962, 2021.
15) Zhu Q, Huang L, Yang Q, Ao Z, Yang R: Metabolomic analysis of exosomal-markers in esophageal squamous cell carcinoma. *Nanoscale* 13(39): 16457−16464, 2021.

16) Peterka O, Jirásko R, Chocholoušková M, Kuchař L, Wolrab D, et al: Lipidomic characterization of exosomes isolated from human plasma using various mass spectrometry techniques. *Biochim Biophys Acta Mol Cell Biol Lipids* 1865(5): 158634, 2020.
17) Fan TWM, Zhang X, Wang C, Yang Y, Kang WY, et al: Exosomal lipids for classifying early and late stage non-small cell lung cancer. *Anal Chim Acta* 1037: 256−264, 2018.
18) Nakai W, Yoshida T, Diez D, Miyatake Y, Nishibu T, et al: A novel affinity-based method for the isolation of highly purified extracellular vesicles. *Sci Rep* 6: 33935, 2016.
19) Sarafian MH, Gaudin M, Lewis MR, Martin FP, Holmes E et al: Objective set of criteria for optimization of sample preparation procedures for ultra-high throughput untargeted blood plasma lipid profiling by ultra performance liquid chromatography-mass spectrometry. *Anal Chem* 86(12): 5766−5774, 2014.
20) Durbin BP, Hardin JS, Hawkins DM, Rocke DM: A variance-stabilizing transformation for gene-expression microarray data. *Bioinformatics* 18 Suppl 1: S105−110, 2002.
21) Liakh I, Sledzinski T, Kaska L, Mozolewska P, Mika A: Sample preparation methods for lipidomics approaches used in studies of obesity. *Molecules* 25(22): 5307, 2020.
22) Bligh EG, Dyer WJ: A rapid method of total lipid extraction and purification. *Can J Biochem Physiol* 37: 911−917, 1959.
23) Want EJ, Masson P, Michopoulos F, Wilson ID, Theodoridis G, et al: Global metabolic profiling of animal and human tissues via UPLC-MS. *Nat Protoc* 8(1): 17−32, 2013.
24) Saigusa D, Okamura Y, Motoike IN, Katoh Y, Kurosawa Y, et al: Establishment of protocols for global metabolomics by LC-MS for biomarker discovery. *PLoS One* 11(8): e0160555, 2016.
25) Uranbileg B, Ito N, Kurano M, Saigusa D, Saito R, et al: Alteration of the lysophosphatidic acid and its precursor lysophosphatidylcholine levels in spinal cord stenosis: A study using a rat cauda equina compression model. *Sci Rep* 9(1): 16578, 2019.
26) Yoshioka K, Hirakawa Y, Kurano M, Ube Y, Ono Y, et al: Lysophosphatidylcholine mediates fast decline in kidney function in diabetic kidney disease. *Kidney Int* 101(3): 510−526, 2022.
27) Wojakowska A, Zebrowska A, Skowronek A, Rutkowski T, Polanski K, et al: Metabolic profiles of whole serum and serum-derived exosomes are different in head and neck cancer patients treated by radiotherapy. *J Pers Med* 10(4): 229, 2020.
28) Okazaki K, Papagiannakopoulos T, Motohashi H: Metabolic features of cancer cells in NRF2 addiction status. *Biophys Rev* 12(2): 435−441, 2020.
29) Barter PJ, Kastelein JJ: Targeting cholesteryl ester transfer protein for the prevention and management of cardiovascular disease. *J Am Coll Cardiol* 47(3): 492−9, 2006.
30) Schumacher F, Carpinteiro A, Edwards MJ, Wilson GC, Keitsch S, et al: Stress induces major depressive disorder by a neutral sphingomyelinase 2-mediated accumulation of ceramide-enriched exosomes in the blood plasma. *J Mol Med (Berl)* 100(10): 1493−1508, 2022.
31) Obata Y, Kita S, Koyama Y, Fukuda S, Takeda H, et al: Adiponectin/T-cadherin system enhances exosome biogenesis and decreases cellular ceramides by exosomal release. *JCI Insight* 3(8): e99680, 2018.
32) Kosaka N, Iguchi H, Hagiwara K, Yoshioka Y, Takeshita F, et al: Natural sphingomyelinase 2 (nSMase2)-dependent exosomal transfer of angiogenic microRNAs regulate cancer cell metastasis. *J Biol Chem* 288(15): 10849−10859, 2013.
33) Chen S, Datta-Chaudhuri A, Deme P, Dickens A, Dastgheyb R, et al: Lipidomic characterization of extracellular vesicles in human serum. *J Circ Biomark* 8: 1849454419879848, 2019.
34) Guo M, Yin Z, Chen F, Lei P: Mesenchymal stem cell-derived exosome: A promising alternative in the therapy of Alzheimer's disease. *Alzheimers Res Ther* 12(1): 109, 2020.
35) Ishizuka K, Kon K, Lee-Okada HC, Arai K, Uchiyama A, et al: Aging exacerbates high-fat diet-induced steatohepatitis through alteration in hepatic lipid metabolism in mice. *J Gastroenterol Hepatol* 35(8): 1437−1448, 2020.
36) Saigusa D, Hishinuma E, Matsukawa N, Takahashi M, Inoue J, et al: Comparison of kit-based metabolomics with other methodologies in a large cohort, towards establishing reference values. *Metabolites* 11(10): 652, 2021.